

Applying the Maximum Entropy Technique to the Gaussian Dispersion Plume Model

J.A. Secrest¹, J.M. Conroy² and H.G. Miller²

¹*Department of Physics and Astronomy, Georgia Southern University,
Armstrong Campus, Savannah, Georgia, USA and*

²*Department of Physics, State University of New
York at Fredonia, Fredonia, New York, USA*

(Dated: October 23, 2020)

Abstract

The Maximum Entropy (MaxEnt) technique is applied to the derivation of the Gaussian Dispersion Plume Model as well as to more complex transport phenomena such as the one-dimensional advection equation, the one-dimensional diffusion equation, the one dimensional advection-diffusion equation, and finally to the multi-dimensional advection-diffusion equation. Further application is discussed.

I. INTRODUCTION

The transport of contaminants due to advective and diffusive processes in the environmental media from the emission of pollutant sources is a concern to many. One of the most ubiquitous air pollution models is the Gaussian Dispersion Plume Model (GDPM). This note focuses on the development of a deeper understanding of this venerable yet highly robust model via the Maximum Entropy Principle. The GDPM is a mathematical model that utilizes a Gaussian distribution to describe temporal and spatial turbulent diffusive and advective concentration spread of the pollutants from a number of sources constrained by initial and boundary conditions.. This model has been applied to a wide number of situations such as the release of smoke from wildfires [1, 2], carbon dioxide from volcanoes [3], radionuclides from the Fukushima and Chernobyl nuclear accidents [4–6], chemical or biological agents[7–11] in the atmosphere in response to various meteorological conditions. These models are widely used by numerous agencies such as the United States’ Environmental Protection Agency (EPA) [12], National Oceanic and Atmospheric Administration (NOAA) [13], the Department of Defence (DoD) [14] as well as numerous private industries.

a. Outline The GDPM is based on the Gaussian distribution and as such will be discussed first. The mathematics of the model will be examined in detail. The Maximum Entropy concept will be introduced as well a generalized analytic solution derived from the paradigm. This maximum entropy solution will then be applied to various transport phenomena such as the advection and advection-diffusion equations in one and several dimensions. The results from these applications will then be applied to the full GDPM which will be derived from first principles. The results will be analysed along with experimental techniques to refine the model.

II. THE IMPORTANCE OF BEING GAUSSIAN

The Gaussian distribution, also known as the normal distribution, the central distribution, and the bell curve due to its familiar shape resembling that of a bell, is a pervasive probability density distribution (pdf), $p(x)$ that yields the expected frequency of an outcome as a function of some variable x . This distribution can be found in a myriad of subjects such as physics, economics, biology, mathematics, statistics etc. This ever-present distribution is

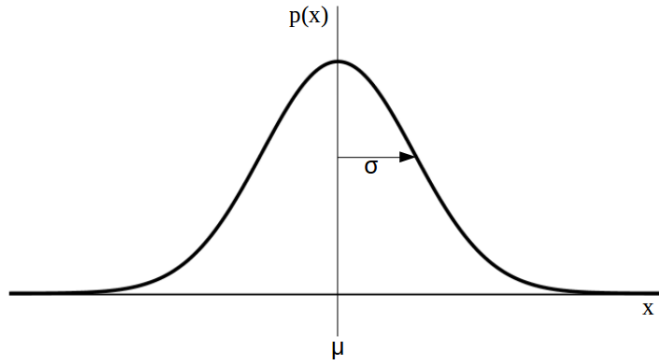


FIG. 1: An example of a Gaussian distribution. The center of the distribution is given by the average μ and the width of the distribution is given by the square root of the variance (standard deviation) σ .

found nearly everywhere for a number of reasons that will be examined below.

The Gaussian distribution is symmetric and resembles that of the bell curve and is often described by this phrase. Mathematically the Gaussian distribution, in one-dimension, is described by

$$p(x) = \frac{1}{\sqrt{2\pi\sigma^2}} e^{-\frac{1}{2} \frac{(x-\mu)^2}{\sigma^2}}, \quad (1)$$

where σ is the standard deviation, μ is the mean, and x is the independent variable corresponding to the probability of $p(x)$ (see Figure 1). The Gaussian distribution has a number of mathematically attractive traits such as:

- the mean, median, and mode are the same,
- the distribution is symmetric about the average $x = \mu$,
- the distribution is completely described by two moments,
- even ordered higher moments are related to standard deviation and mean,
- the product of Gaussian distributions is again a Gaussian distribution,
- the convolution of Gaussian distributions is again a Gaussian distribution,
- the Fourier transform of a Gaussian is again a Gaussian,
- the sum of Gaussian distributions is again a Gaussian distribution.

The Gaussian distribution is a result of the central limit theorem. In essence, this theorem states that as the number of trial samples becomes large, the probability distribution approaches that of the Gaussian distribution. In many situations there are a number of independent random variables that follow some distribution law themselves. Each of these independent trials are sampled from their own distribution and then combine to form the overall Gaussian distribution. This could be thought of intuitively as the sum of Gaussian distributions simply yield another Gaussian. The Gaussian, $y = e^{-ax^2}$, also appears as a solution to differential equations of the form

$$\frac{dy}{dx} + 2axy = 0. \quad (2)$$

This class of differential equations occurs when the rate of change of some quantity can be related back to itself. Examples of this kind of relationship can be found in radioactivity, material cooling, population dynamics, and interest from bank accounts.

Due to the robustness of the Gaussian distribution, even distributions that are not Gaussian can many times be approximated by this distribution. Discrete distributions like the binomial and Poisson distributions will asymptotically approach the Gaussian distribution, as will continuous distributions like log-normal, Rayleigh, Gamma, Laplace, chi-square, and student t- distributions. Again, this is due to the central limit theorem described above. Given a sufficiently large number of random events with some variance and mean, the result will become Gaussian distributed.

III. THE MATHEMATICAL MODEL

Pollution in the atmosphere is essentially described by a conservation law for the suspended particles in the environmental media. This combination of conservation of mass and the advection-diffusion equation describing turbulent diffusion can be written as,

$$\frac{\partial C}{\partial t} + \vec{\nabla} \cdot (\vec{u}C) = \vec{\nabla} \cdot (K\vec{\nabla}C), \quad (3)$$

where C is the concentration, $\vec{u} = (u, v, w)$ is the average wind velocity with components in the x-,y-, and z-directions respectively, and $K = (K_x, K_y, K_z)$ is the eddy diffusivity with components in the x-,y-, and z-directions respectively. Assuming the medium is incompressible and the divergence operator can be expanded such that $\vec{\nabla} \cdot \vec{u} = 0$, Eqn 3 can be written

as,

$$\frac{\partial C}{\partial t} + u \frac{\partial C}{\partial x} + v \frac{\partial C}{\partial y} + w \frac{\partial C}{\partial z} = \frac{\partial}{\partial x} \left(K_x \frac{\partial C}{\partial x} \right) + \frac{\partial}{\partial y} \left(K_y \frac{\partial C}{\partial y} \right) + \frac{\partial}{\partial z} \left(K_z \frac{\partial C}{\partial z} \right). \quad (4)$$

It should be noted that the wind velocity and concentration are made up of two components,

$$\vec{u} = \vec{u}_{avg} + \vec{u}_{fluct} \quad (5)$$

and

$$C = C_{avg} + C_{fluct}, \quad (6)$$

associated with the average (avg) and fluctuating (fluct) components of the parameter being examined. It is assumed that the fluctuations cancel out on large enough time scales and ignore their contribution.

The bulk motion in the x -direction dominates over the contribution from the corresponding diffusion term in the same direction and so the diffusion term is neglected. It is assumed that the wind speeds in the y - and z - directions are minimal in comparison to the wind speed in x and so they are neglected. This yields,

$$\frac{\partial C}{\partial t} + u \frac{\partial C}{\partial x} = \frac{\partial}{\partial y} \left(K_y \frac{\partial C}{\partial y} \right) + \frac{\partial}{\partial z} \left(K_z \frac{\partial C}{\partial z} \right). \quad (7)$$

where the x -direction is the direction of wind current (along-wind), the y -direction is the cross-wind direction, the z -direction is the vertical direction measured from the ground, C is the concentration of the pollutant, K_y and K_z are the diffusivity in the x and y -directions, and u is the mean wind velocity along the x -axis. Assuming that the diffusivity constants are indeed constant leads to the equations

$$\frac{\partial C}{\partial t} + u \frac{\partial C}{\partial x} = K_y \frac{\partial^2 C}{\partial y^2} + K_z \frac{\partial^2 C}{\partial z^2}. \quad (8)$$

The boundary conditions are:

- the source concentration is given as $C(0, y, z) = \frac{Q}{u} \delta(y) \delta(z - H)$ where Q is the concentration rate from a source located at a height $z = H$ at position $x = 0$ and advected at a velocity u in the x -direction,
- $C(x, \pm\infty, z) = 0$,
- $C(\infty, y, z) = 0$
- $C(x, y, \infty) = 0$,

- and $K_z \frac{\partial C}{\partial z}(x, y, 0) = 0$ which is a statement that the ground is reflecting.

This yields the celebrated solution along with the boundary conditions, defining the standard deviation, σ , in terms of the diffusivity constant and time as $\sigma^2 = 2Kt$,

$$C(x, y, z) = \frac{Q}{2\pi u \sigma_y \sigma_x} \left[e^{-\frac{y^2}{2\sigma_y^2}} \right] \left(e^{-\frac{(z-H)^2}{2\sigma_z^2}} + e^{-\frac{(z+H)^2}{2\sigma_z^2}} \right), \quad (9)$$

where x is the downwind distance, y is the crosswind distance, z is the vertical distance from the ground, Q is the contaminant emission rate, σ_y is the lateral dispersion function, σ_z is the vertical dispersion function, and H is the effective stack height.

It should be noted that the effective stack height is made up of two contributions,

$$H = h + \delta h_{pr} \quad (10)$$

where h is the actual stack height and δh_{pr} is the effective plume rise above the top of the smoke stack.

It should also be noted that Eq. 9 reduces to the solution for an emission point source at ground level without an effective plume rise,

$$C(x, y, z) = \frac{Q}{\pi u \sigma_y \sigma_x} e^{-\frac{1}{2} \left(\frac{y^2}{\sigma_y^2} + \frac{z^2}{\sigma_z^2} \right)} \quad (11)$$

where the parameters are defined as above.

IV. THE MAXIMUM ENTROPY PRINCIPLE

Entropy may simply be regarded as an information measure for a system. The MaxEnt principle finds its roots in Laplace's principle of insufficient reason (or sometimes referred to as indifference) which states that, given no additional information, it is reasonable to choose a uniform probability distribution. The MaxEnt principle takes this to its natural conclusion and suggests that the probability distribution is the least biased distribution given the known constraints.

Jaynes [15, 16] suggested that the most likely probability distribution function should be one that obeys the known constraints (the moments) while maximizing the entropy. This is known as the maximum entropy (MaxEnt) method. This technique minimizes the amount of relevant prior information that is used to determine the distribution function while allowing

the distribution to evolve towards maximal entropy. This idea of finding the least biased distribution with the known data as constraints is highly appealing.

It should be noted that Maximum Entropy techniques have been applied to a wide variety of subjects. In physics, this technique has been used in particle physics to determine the quark distribution in pions [17], QCD calculations [18], in condensed matter physics applications such as solving certain mathematical techniques [19] and the modeling of Helium-4 [20] and in astronomy the principle has been used to aid in the reconstruction of x-ray images [21, 22] and in the analysis of the mass-radius relationship of exo-planets [23], as well as providing a unified view of transport equations (ref our paper). In biology it has been used to analyse the structure of DNA [24–26], model species distributions [24, 27–29], and to study gene expression [30, 31]. The method has even been applied to understanding economic growth in a myriad of settings [32–34].

The constraints, which represent the limited amount of information known, may be the moments of the probability distribution function [35]. These constraints can be experimentally determined. Analytically, the n^{th} moment, μ_n , depending on a physical observable ξ for a probability distribution function $\rho(\xi)$ is defined as

$$\langle \xi^n \rangle = \int_{-\infty}^{\infty} \xi^n \rho(\xi) d\xi. \quad (12)$$

It should be noted that the zeroth moment, $\langle 1 \rangle$ is the normalization. The Shannon-Kullback information entropy is defined as [36] the weighted average of the log of the probabilities,

$$S = - \int_{-\infty}^{\infty} \rho(\xi) \ln \frac{\rho(\xi)}{\rho_0(\xi)} d\xi, \quad (13)$$

where ρ_0 is an invariant measure. The maximum entropy principle states that the most likely probability distribution will be one that maximizes the entropy subject to the known constraints. The constraints are imposed via Lagrange's multipliers (which may have time dependence) λ_0, λ_1 , and λ_2 ,

$$\begin{aligned} S = & - \int_{-\infty}^{\infty} \rho(\xi) \ln \frac{\rho(\xi)}{\rho_0(\xi)} d\xi \\ & - (\lambda_0 - 1) \left[\int_{-\infty}^{\infty} \rho(\xi) d\xi - \langle 1 \rangle \right] \\ & - \lambda_1 \left[\int_{-\infty}^{\infty} \xi \rho(\xi) d\xi - \langle \xi^1 \rangle \right] \\ & - \lambda_2 \left[\int_{-\infty}^{\infty} \xi^2 \rho(\xi) d\xi - \langle \xi^2 \rangle \right]. \end{aligned} \quad (14)$$

Variational calculus is used in order to maximize Eq. (14) within the bounds of the constraints,

$$\delta S = 0, \quad (15)$$

and solving for the probability distribution yields

$$\rho = \rho_0(\xi)e^{-\lambda_2\xi^2 - \lambda_1\xi - \lambda_0}. \quad (16)$$

This yields a generic solution to the MaxEnt problem. One must determine the Lagrange multipliers from the equations of constraint in order to determine the particular solution at hand.

If the time derivatives of the equations of constraint constitute a closed set of differential equations the static solution may be viewed as the solution to the MaxEnt equations at a given time and the time dependent solutions are obtained by replacing λ_i by $\lambda_i(t)$ which satisfy the time dependent equations of constraint ([37]).

V. APPLICATION OF MAXIMUM ENTROPY PRINCIPLE TO ONE-DIMENSIONAL ADVECTION

The advection equation [38] is a hyperbolic partial differential equation of the form

$$\frac{\partial \rho(x, t)}{\partial t} + v \frac{\partial \rho(x, t)}{\partial x} = 0 \quad (17)$$

that describes how a scalar field density f is swept along (advected) by a bulk flow of constant speed v . The position $-\infty < x < \infty$, the time $0 < t < \infty$, and the velocity field v are nonzero. Examples of where the advection equation is used are modeling automobile traffic[39, 40], blood flow through a capillary [41, 42], and salinity propagation in the ocean [44, 45].

It is well known that the exact form of the solution to this partial differential equation has the form $\rho(x, t) = \rho(x - vt, 0)$. This means that the probability distribution function does not change its initial shape during advection.

Lets apply the MaxEnt method to solve the advection equation, Eq. 17, to determine the particular solution,

$$\rho(x, t) = \frac{1}{\sqrt{2\pi\sigma^2}} e^{-\frac{1}{2} \frac{(x-vt)^2}{\sigma^2}}. \quad (18)$$

given the initial condition of a Gaussian profile $\rho_0(x, 0) = \frac{1}{\sqrt{2\pi\sigma^2}}e^{-\frac{1}{2}x^2}$.

The advection equation is rearranged,

$$\frac{\partial\rho(x, t)}{\partial t} = -v\frac{\partial\rho(x, t)}{\partial x} \quad (19)$$

and integrated spatially over x on both sides of the equation,

$$\int_{-\infty}^{\infty} \frac{\partial\rho(x, t)}{\partial t} dx = - \int_{-\infty}^{\infty} v\frac{\partial\rho(x, t)}{\partial x} dx. \quad (20)$$

Assuming that the derivative operator can be removed from under the spatial integral along with the constant velocity,

$$\frac{d}{dt} \int_{-\infty}^{\infty} \rho(x, t) dx = -v \int_{-\infty}^{\infty} \frac{\partial\rho(x, t)}{\partial x} dx, \quad (21)$$

it is noted that the integral on the left is the zeroth moment, the normalization, and that the integral on the right yields zero due to the boundary conditions imposed on the probability distribution function. This simply yields,

$$\frac{d\langle 1 \rangle}{dt} = 0 \quad (22)$$

which is just the statement that the zeroth moment, i.e. the normalization, is a constant (usually taken to be one),

$$\langle 1 \rangle = 1. \quad (23)$$

Again, applying the same idea to Eq.(19), but this time multiplying both sides by x and integrating,

$$\int_{-\infty}^{\infty} \frac{\partial\rho(x, t)}{\partial t} x dx = - \int_{-\infty}^{\infty} v\frac{\partial\rho(x, t)}{\partial x} x dx, \quad (24)$$

assuming that the temporal derivative operator can be removed from the integral on the left and integrating-by-parts on the right yields,

$$\frac{d}{dt} \int_{-\infty}^{\infty} \rho x dx = -v \left[x\rho \Big|_{-\infty}^{\infty} - \int_{-\infty}^{\infty} \rho dx \right], \quad (25)$$

where the surface goes to zero due to the boundary conditions imposed on the probability distribution function, ρ , the integral on the right hand side is identified with the first spatial moment, $\langle x \rangle$, and the remaining integral on the right is identified with the zeroth moment, the normalization $\langle 1 \rangle$. Note that the differential equations for the moments are a closed set.

Finally this results in

$$\frac{d\langle x \rangle}{dt} = v. \quad (26)$$

This is integrated to determine the temporal dependence of the first moment,

$$\langle x \rangle = vt. \quad (27)$$

The moments are calculated from the MaxEnt solution are:

$$\langle 1 \rangle = \int_{-\infty}^{\infty} \rho_0(x) e^{-\lambda_2 x^2 - \lambda_1 x - \lambda_0} = \int_{-\infty}^{\infty} \frac{1}{\sqrt{2\pi\sigma^2}} e^{-\frac{1}{2}x^2} e^{-\lambda_1 x - \lambda_0} = e^{-\lambda_0} e^{\frac{\lambda_1^2 \sigma^2}{2}}, \quad (28)$$

and

$$\langle x \rangle = \int_{-\infty}^{\infty} x \rho_0(x) e^{-\lambda_2 x^2 - \lambda_1 x - \lambda_0} = \int_{-\infty}^{\infty} x \frac{1}{\sqrt{2\pi\sigma^2}} e^{-\frac{1}{2}x^2} e^{-\lambda_1 x - \lambda_0} = -\lambda_1 \sigma^2 e^{-\lambda_0} e^{\frac{\lambda_1^2 \sigma^2}{2}}. \quad (29)$$

Equating the moments from Eqs. (23) and (28) and Eqs. (27) and (29) and solving for the Lagrange multipliers, $\lambda_0 = \lambda_0(t) = \frac{(vt)^2}{2\sigma^2}$ and $\lambda_1 = \lambda_1(t) = -\frac{vt}{\sigma^2}$. Substituting these results back into the MaxEnt solution Eq. (16) results in the solution given by Eq. (18).

VI. APPLICATION OF MAXIMUM ENTROPY PRINCIPLE TO ONE-DIMENSIONAL DIFFUSION

Consider the one-dimensional diffusion equation with constant eddy diffusivity constant K is given by

$$\frac{\partial \rho}{\partial t} = K \frac{\partial^2 \rho}{\partial x^2}, \quad (30)$$

where ρ is the probability distribution function that obeys the boundary conditions that as x approaches $\pm\infty$, $\rho \rightarrow 0$ with the initial condition that $\rho(x, t) = \rho(x, 0) = \rho_0$. This results in the celebrated Gaussian solution,

$$\rho = \frac{\rho_0}{\sqrt{2\pi\sigma}} e^{-\frac{1}{2}\left(\frac{x}{\sigma}\right)^2}. \quad (31)$$

Integrating both sides of Eq. (30),

$$\int_{-\infty}^{\infty} \frac{\partial \rho}{\partial t} dx = K \int_{-\infty}^{\infty} \frac{\partial^2 \rho}{\partial x^2} dx, \quad (32)$$

pulling out the temporal derivative operator and noting the integral on the left hand side is the zeroth moment of the probability distribution function, $\int_{-\infty}^{\infty} \rho dx = \langle 1 \rangle$,

$$\frac{d\langle 1 \rangle}{dt} = \frac{\partial \rho}{\partial x} \Big|_{-\infty}^{\infty} = 0 \quad (33)$$

simply yields the normalization condition,

$$\langle 1 \rangle = 1. \quad (34)$$

Multiplying both sides by the position x , integrating in order to exploit the first moment,

$$\frac{d}{dt} \int_{-\infty}^{\infty} x \rho dx = K \int_{-\infty}^{\infty} x \frac{\partial^2 \rho}{\partial x^2} dx \quad (35)$$

, noting that the integral on the left is the average position, $\langle x \rangle$, and integrating by parts on the right hand side gives

$$\frac{d\langle x \rangle}{dt} = K \left[x \frac{\partial \rho}{\partial x} \Big|_{-\infty}^{\infty} - \int_{-\infty}^{\infty} \frac{\partial \rho}{\partial x} dx \right] = 0 \quad (36)$$

It is seen that the average position in the x -direction is a constant. This is to be expected for a symmetric distribution starting at $x = 0$.

Applying this technique again to Eq. (30) by multiplying both sides by x^2 and integrating over all space to exploit the second position moment gives

$$\frac{d}{dt} \int_{-\infty}^{\infty} x^2 \rho dx = K \int_{-\infty}^{\infty} x^2 \frac{\partial^2 \rho}{\partial x^2} dx. \quad (37)$$

Again noting that the left hand side is the second moment and using integration-by-parts on the right hand side results in

$$\frac{d\langle x^2 \rangle}{dt} = K \left[x^2 \frac{\partial \rho}{\partial x} \Big|_{-\infty}^{\infty} - \int_{-\infty}^{\infty} 2x \frac{\partial \rho}{\partial x} dx \right] \quad (38)$$

and integrating the second integral by parts yields

$$\frac{d\langle x^2 \rangle}{dt} = K \left[-2 \left(\rho x \Big|_{-\infty}^{\infty} - \int_{-\infty}^{\infty} \rho dx \right) \right] \quad (39)$$

$$= 2K \langle \rho \rangle. \quad (40)$$

Integrating, applying the initial conditions, and solving for the second moment results in

$$\langle x^2 \rangle = 2Kt. \quad (41)$$

Knowing that the solution from Eq. (16) has the form

$$\rho = \rho_0 e^{-\lambda_2 x^2 - \lambda_0}, \quad (42)$$

for the initial condition ρ_0 , one can use the constraints and the generic solution to determine the undetermined multipliers. From the normalization

$$\langle 1 \rangle = \int_{-\infty}^{\infty} \rho dx = \int_{-\infty}^{\infty} \rho_0 e^{-\lambda_2 x^2 - \lambda_0} = \rho_0 e^{-\lambda_0} \left[\frac{\sqrt{\pi}}{\sqrt{\lambda_2}} \right] = 1 \quad (43)$$

and the second moment along with the result

$$\langle x^2 \rangle = \int_{-\infty}^{\infty} x^2 \rho dx = \rho_0 e^{-\lambda_0} \int_{-\infty}^{\infty} x^2 e^{-\lambda_2 x^2} dx = \rho_0 e^{-\lambda_0} \left[\frac{\sqrt{\pi}}{2\lambda_2^{\frac{5}{2}}} \right] = 2\rho_0 K t \quad (44)$$

one finds $e^{-\lambda_0} = \frac{\sqrt{\lambda_2}}{\sqrt{\pi}}$ and $\lambda_2 = \frac{1}{4Kt}$, which yields the well-known solution

$$\rho = \frac{\rho_0}{\sqrt{4\pi K t}} e^{-\frac{x^2}{4Kt}}. \quad (45)$$

Typically this is in terms of the standard deviation $\sigma = \sqrt{2Kt}$, which is the solution given by Eq. (31).

In the above example, the diffusive process is centered around the origin, $x = 0$. The probability distribution can be translated to a different center, x_0 by replacing x with $x - x_0$, which amounts to replacing Eq. (31) with

$$\rho = \frac{\rho_0}{\sqrt{2\pi\sigma}} e^{-\frac{(x-x_0)^2}{2\sigma^2}}. \quad (46)$$

Note that the solutions to the advection equation and the diffusion equation look remarkably similar. The results of the advection equation were with the initial condition that the probability distribution function was a Gaussian distribution. Then as time moved forward the solution is simply the same shape of the initial distribution but translated (or better said, advected) along the x -axis. The solution for the diffusion equation is the Gaussian distribution centered around its initial position (in this case $x = 0$), an initial condition was not given and it should be noted that the distribution widens as time increases. Hence the solutions may appear the same at first but the origin of the two solutions is different, as are the subsequent characteristics of each.

VII. APPLICATION OF MAXIMUM ENTROPY PRINCIPLE TO ONE-DIMENSIONAL ADVECTION-DIFFUSION MODEL

The one-dimensional advection-diffusion equation is given by

$$\frac{\partial \rho}{\partial t} + v \frac{\partial \rho}{\partial x} = K \frac{\partial^2 \rho}{\partial x^2}, \quad (47)$$

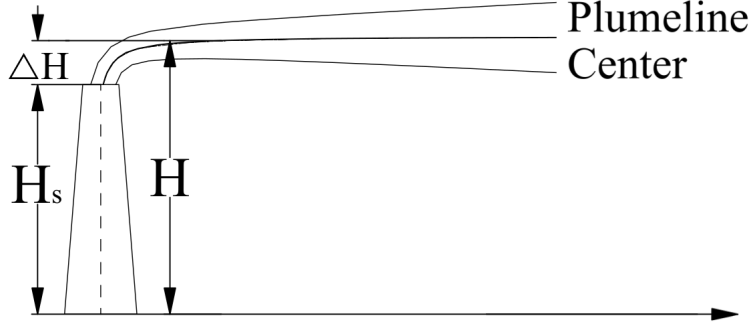


FIG. 2: The point source for emission is given by the height of the smoke stack. The plume is advected horizontally along the plumeline center as the width of the smokeplume grows due to diffusion.

where ρ is the probability density function, v is the advective velocity, and K is the eddy diffusion constant (see Figure 2). Integrating both sides of Eq. (47) by x ,

$$\frac{d}{dt} \int_{-\infty}^{\infty} \rho dx + v \int_{-\infty}^{\infty} \frac{\partial \rho}{\partial x} dx = K \int_{-\infty}^{\infty} \frac{\partial^2 \rho}{\partial x^2} dx, \quad (48)$$

yields the result

$$\frac{d}{dt} \langle 1 \rangle = 0, \quad (49)$$

implying that the normalization is a constant. Again multiplying by x and integrating Eq. (47) gives

$$\frac{d}{dt} \int_{-\infty}^{\infty} x \rho dx + v \int_{-\infty}^{\infty} x \frac{\partial \rho}{\partial x} dx = K \int_{-\infty}^{\infty} x \frac{\partial^2 \rho}{\partial x^2} dx. \quad (50)$$

Integrating by parts leads to

$$\frac{d}{dt} \langle x \rangle + \left[x \rho \Big|_{-\infty}^{\infty} - \int_{-\infty}^{\infty} \rho dx \right] = K \left[x \frac{\partial \rho}{\partial x} \Big|_{-\infty}^{\infty} - \int_{-\infty}^{\infty} \frac{\partial \rho}{\partial x} dx \right], \quad (51)$$

where the surface terms go to zero due to the boundary conditions. After integrating over time, this leads to

$$\langle x \rangle = vt. \quad (52)$$

Multiplying Eq. (47) by x^2 to obtain an equation in terms of the second moment and integrating leads to

$$\frac{d}{dt} \int_{-\infty}^{\infty} x^2 \rho dx + u \int_{-\infty}^{\infty} x^2 \frac{\partial \rho}{\partial x} dx = K \int_{-\infty}^{\infty} x^2 \frac{\partial^2 \rho}{\partial x^2} dx. \quad (53)$$

Again, integrating by parts yields

$$\frac{d}{dt} \langle x^2 \rangle + \left[x^2 \rho \Big|_{-\infty}^{\infty} - 2 \int_{-\infty}^{\infty} x \rho dx \right] = K \left[x^2 \frac{\partial \rho}{\partial x} \Big|_{-\infty}^{\infty} - 2 \int_{-\infty}^{\infty} x \frac{\partial \rho}{\partial x} dx \right]. \quad (54)$$

Again, the surface terms go to zero. Applying integration by parts to the last integral on the right hand side leads to

$$\frac{d}{dt}\langle x^2 \rangle - 2v\langle x \rangle = K \left[-2 \left(x\rho \Big|_{-\infty}^{\infty} - \int_{-\infty}^{\infty} \rho dx \right) \right]. \quad (55)$$

Using the result from Eq. (52) and integrating over time yields

$$\langle x^2 \rangle = 2Kt + v^2t^2. \quad (56)$$

Using the MaxEnt solution of Eq. (16) to find the zeroth, first, and second moments, and equating to Eqs. (49), (52), and (56), results in

$$\langle 1 \rangle = \int_{-\infty}^{\infty} \rho dx = \int_{-\infty}^{\infty} \rho_0 e^{-\lambda_2 x^2 - \lambda_1 x - \lambda_0} = \rho_0 e^{-\lambda_0} \left[\frac{e^{\frac{\lambda_1^2}{4\lambda_2}} \sqrt{\pi}}{\sqrt{\lambda_2}} \right] = 1, \quad (57)$$

$$\langle x \rangle = \int_{-\infty}^{\infty} x^2 \rho dx = \rho_0 \int_{-\infty}^{\infty} x e^{-\lambda_2 x^2 - \lambda_1 x - \lambda_0} dx = -\rho_0 e^{-\lambda_0} \left[\frac{\lambda_1 e^{\frac{\lambda_1^2}{4\lambda_2}} \sqrt{\pi}}{4\lambda_2^{\frac{3}{2}}} \right] = vt, \quad (58)$$

and

$$\langle x^2 \rangle = \int_{-\infty}^{\infty} x^2 \rho dx = \rho_0 \int_{-\infty}^{\infty} x^2 e^{-\lambda_2 x^2 - \lambda_1 x - \lambda_0} dx = \rho_0 e^{-\lambda_0} \left[(2\lambda_2 + \lambda_1^2) \frac{e^{\frac{\lambda_1^2}{4\lambda_2}} \sqrt{\pi}}{4\lambda_2^{\frac{5}{2}}} \right] = 2Kt + v^2t^2. \quad (59)$$

Solving for the Lagrange multipliers leads to $e^{-\lambda_0} = \frac{1}{\sqrt{4\pi Kt}} e^{-\frac{v^2 t^2}{4Kt}}$, $\lambda_1 = \frac{v}{2K}$, and $\lambda_2 = \frac{1}{4Kt}$. Finally, this leads to the result that the probability distribution function is

$$\frac{\rho_0}{\sqrt{4\pi Kt}} e^{-\frac{(x-vt)^2}{4Kt}}, \quad (60)$$

which is the combination of the advection and diffusion equation solutions Eqs. (18) and (31) in one dimension that were solved in Sections V and VI.

VIII. APPLICATION OF MAXIMUM ENTROPY PRINCIPLE RESULTS TO THE MULTI-DIMENSIONAL ADVECTION-DIFFUSION MODEL

Using the MaxEnt results from Sections V, VI, and VII, the three dimensional GDPM can be derived. See Fig. 3 for the configuration of the physical system under consideration.

A. Source

The strength of the initial emission Q can be handled in one of two different ways in the model. One method is to add a source term, S and use Dirac delta functions of the form $S = Q\delta(x - x_0)\delta(y - y_0)\delta(z - z_0)$ to Eq. (4). Another method which will be employed in this work will be to use the invariant measure in the MaxEnt solution in Eq. (16). In this case the invariant measure is $\rho = \frac{Q}{u}$ where again, Q is the strength of the emission and u is the downwind speed.

B. Reflection from the Ground

The Gaussian plume that is emitted from some finite height above the ground will eventually spread and encounter the barrier of the ground as the it moves downwind. Since the amount of material must be conserved, the effect of the interaction with the contaminant plume with the ground will cause a reflection effect. Typically in these models the ground is considered a perfect reflector. This ground reflection effect is modeled using the Method of Images [43]. The Method of Images models the reflection by using a virtual source of the strength located the same distance away but below the surface.

C. MaxEnt Solution for the Gaussian Plume Model

The total concentration of pollutant at a given time and location is given by the product of the concentrations in the three directions:

$$C(x, y, z, t) = c_x(x, t)c_y(y, t)c_z(z, t) \quad (61)$$

where $c_x(x, t)$ is the concentration in the x-direction, $c_y(y, t)$ is the concentration in the y-direction, and $c_z(z, t)$ is the concentration in the z-direction. The x-component of the concentration is given by the invariant measure that $\rho = \frac{Q}{u}$. The y-component of the concentration is given by Eq. (31) in Section VI. The z-component is given by the corresponding version of Eq. (31) in Section VI. This yields,

$$C(x, y, z) = \frac{Q}{2\pi u \sigma_y \sigma_x} \left[e^{-\frac{y^2}{2\sigma_y^2}} \right] e^{-\frac{(z-H)^2}{2\sigma_z^2}}. \quad (62)$$

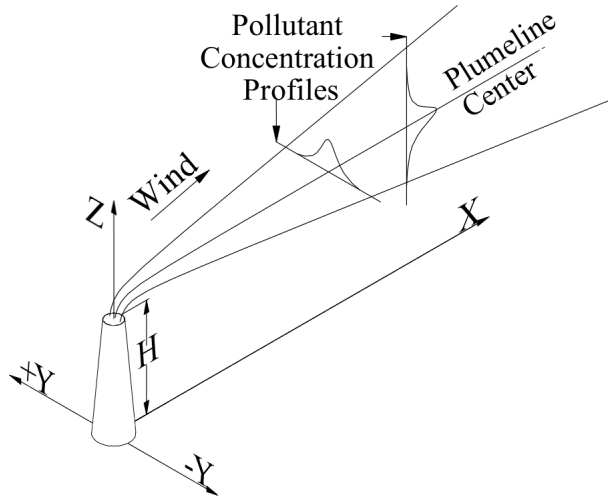


FIG. 3: The smoke plume source along with the concentration profile in the coordinate system under consideration.

Now applying the Methods of Images and utilizing the law of superposition in adding a virtual source below the ground at $z = -H$, yields the result,

$$C(x, y, z) = \frac{Q}{2\pi u \sigma_y \sigma_x} \left[e^{-\frac{y^2}{2\sigma_y^2}} \right] \left(e^{-\frac{(z-H)^2}{2\sigma_z^2}} + e^{-\frac{(z+H)^2}{2\sigma_z^2}} \right), \quad (63)$$

which is in agreement with well-known result quoted in Eq. (9).

IX. A NOVEL WAY TO APPLY THE MAXIMUM ENTROPY PRINCIPLE TO THE GAUSSIAN PLUME MODEL

The GDPM is an excellent example of the application of MaxEnt principle where the information is maximized within the constraints of the situation at hand. These constraints are given by the low-lying moments of the distribution of interest. Since the MaxEnt solution is known, in general, all that must be done in order to determine the particular solution is to determine the constraints via the moments of the distribution. This was recently described by the authors ([35]) where the partial differential equations of interest did not need to be solved. Instead the MaxEnt solution can be used, along with the experimentally determined low-lying moments, to describe the dynamics of the problem.

The GDPM has a long history of doing just that. Experiments have been carried out where concentrations of particulates have been measured at regular intervals depending on

various variables such as rural or urban environments, day or night, and the stability of the atmosphere ([46–49]). Tables of values have been tabulated and often the variance is represented by a power law or other, more sophisticated, parameterizations. These phenomenological models of the low-lying moments are then fed back into the solution in order to yield a realistic representation of the plume dynamics.

X. CONCLUSIONS

The MaxEnt principle was applied to the the advection, diffusion, and the advection-diffusion equations as well as to the advection-diffusion equation along with the appropriate initial and boundary conditions and the GDPM was recovered. This yields a deeper insight into the understanding of the model and its application to continuous release point sources.

Applying the MaxEnt Principle to the model yields a deeper understanding as to why the GDPM works as it does. The fundamental notion is that the probability distribution that one is seeking to model is the one that maximizes the entropy within the given set of constraints in this case the low-lying moments which have been tabulated and parameterized.

The authors do not see any reason that the MaxEnt principle could not be further applied to more complex sources such as line, area, and volume sources and to other models such as the Box Model ([50, 51]), Gaussian Puff Model ([52]), or more complicated numerical models.

A natural extension of this work is to consider different entropic measures. In this work the Shannon entropy was employed but other entropies such as the Tsallis ([53]) and Kaniadakis ([54]) entropy could be investigated for fractional transport equations ([55–57]) to describe the diffusive and advective processes.

XI. BIBLIOGRAPHY

-
- [1] Derek V. Mallia, Adam K. Kochanski, Shawn P. Urbanski, and John C. Lin, *Optimizing smoke and plume rise modeling approaches at local scales*, *Atmosphere* **9** (2018), no. 5.

- [2] Boknam Lee, Seungwan Cho, Seung-Kii Lee, Choongshik Woo, and Joowon Park, *Development of a smoke dispersion forecast system for korean forest fires*, *Forests* **10** (2019), no. 3.
- [3] Xun Jiang and Yuk L. Yung, *Global patterns of carbon dioxide variability from satellite observations*, *Annual Review of Earth and Planetary Sciences* **47** (2019), no. 1, 225–245.
- [4] I. Korsakissok, A. Mathieu, and D. Didier, *Atmospheric dispersion and ground deposition induced by the fukushima nuclear power plant accident: A local-scale simulation and sensitivity study*, *Atmospheric Environment* **70** (2013), 267 – 279.
- [5] Shazmeen Shamsuddin, Nurlyana Omar, and Koh Meng Hock, *Development of radionuclide dispersion modeling software based on gaussian plume model*, *MATEMATIKA* **33** (2017), 149.
- [6] Laila Omar-Nazir, Xiaopei Shi, Anders Moller, Timothy Mousseau, Soohyun Byun, Samuel Hancock, Colin Seymour, and Carmel Mothersill, *Long-term effects of ionizing radiation after the chernobyl accident: Possible contribution of historic dose*, *Environmental Research* **165** (2018), 55 – 62.
- [7] Hiromasa Nakayama and Haruyasu Nagai, *Development of local-scale high-resolution atmospheric dispersion model using large-eddy simulation part 1: Turbulent flow and plume dispersion over a flat terrain*, *Journal of Nuclear Science and Technology* **46** (2009), no. 12, 1170–1177.
- [8] Andron Creary and Walter J. Scott, *Chemical warfare response planning through use of systems engineering casualty analysis simulation*, *Phalanx* **52** (2019), no. 3, 40–47.
- [9] Liang Ma, Bin Chen, Sihang Qiu, Zhen Li, and Xiaogang Qiu, *Agent-based modeling of emergency evacuation in a railway station square under sarin terrorist attack*, *International Journal of Modeling, Simulation, and Scientific Computing* **08** (2017), no. 02, 1750022.
- [10] J. Ray, Y. M. Marzouk, and H. N. Najm, *A bayesian approach for estimating bioterror attacks from patient data*, *Statistics in Medicine* **30** (2011), no. 2, 101–126.
- [11] Lawrence M. Wein, David L. Craft, and Edward H. Kaplan, *Emergency response to an anthrax attack*, *Proceedings of the National Academy of Sciences* **100** (2003), no. 7, 4346–4351.
- [12] United States Environmental Protection Agency, *Guideline on air quality models*, Tech. report, April 1978.
- [13] Roland R. Draxler, *Forty-eight hour atmospheric dispersion forecasts at selected locations in the united states*, NOAA Technical Memorandum ERL ARL-100 (1981).
- [14] United States Department of Defense, *Chapter 13: Specialized radiological monitoring and*

- hazard assessment capabilities*, Tech. report, August 1999.
- [15] E. T. Jaynes, *Information theory and statistical mechanics*, Phys. Rev. **106** (1957), 620–630.
 - [16] E. T. Jaynes, *Information theory and statistical mechanics. ii*, Phys. Rev. **108** (1957), 171–190.
 - [17] Chengdong Han, Hanyang Xing, Xiaopeng Wang, Qiang Fu, Rong Wang, and Xurong Chen, *Pion valence quark distributions from maximum entropy method*, Physics Letters B **800** (2020), 135066.
 - [18] H.-T. Ding, O. Kaczmarek, A.-L. Kruse, R. Larsen, L. Mazur, Swagato Mukherjee, H. Ohno, H. Sandmeyer, and H.-T. Shu, *Charmonium and bottomonium spectral functions in the vector channel*, Nuclear Physics A **982** (2019), 715 – 718.
 - [19] Ryan Levy, J.P.F. LeBlanc, and Emanuel Gull, *Implementation of the maximum entropy method for analytic continuation*, Computer Physics Communications **215** (2017), 149 – 155.
 - [20] Youssef Kora and Massimo Boninsegni, *Dynamic structure factor of superfluid ^4He from quantum monte carlo: Maximum entropy revisited*, Phys. Rev. B **98** (2018), 134509.
 - [21] R. Willingale, *Use of the maximum entropy method in X-ray astronomy*, Monthly Notices of the Royal Astronomical Society **194** (1981), no. 2, 359–364.
 - [22] Ju Guan, Li-Ming Song, and Zhuo-Xi Huo, *Application of a multiscale maximum entropy image restoration algorithm to HXMT observations*, Chinese Physics C **40** (2016), no. 8, 086203.
 - [23] Qi Ma and Sujit K. Ghosh, *Maximum entropy-based probabilistic mass–radius relation of exoplanets*, The Astronomical Journal **158** (2019), no. 2, 86.
 - [24] Ronald M. Levy, *Insights into the energy landscapes of chromosome organization proteins from coevolutionary sequence variation and structural modeling*, Proceedings of the National Academy of Sciences (2020).
 - [25] Céline Trébeau, Jacques Boutet de Monvel, Fabienne Wong Jun Tai, Christine Petit, and Raphaël Etournay, *DNABarcodeCompatibility: an R-package for optimizing DNA-barcode combinations in multiplex sequencing experiments*, Bioinformatics **35** (2018), no. 15, 2690–2691.
 - [26] Gene Yeo and Christopher B. Burge, *Maximum entropy modeling of short sequence motifs with applications to rna splicing signals*, Journal of Computational Biology **11** (2004), no. 2-3, 377–394.
 - [27] Roger Baldwin, *Use of maximum entropy modeling in wildlife research*, Entropy **11** (2009),

- no. 4, 854–866.
- [28] Mohsen Kalboussi and Hammadi Achour, *Modelling the spatial distribution of snake species in northwestern tunisia using maximum entropy (maxent) and geographic information system (gis)*, *Journal of Forestry Research* **29** (2018), no. 1, 233–245.
- [29] Lifei Wang, Lisa A. Kerr, Nicholas R. Record, Eric Bridger, Benjamin Tupper, Katherine E. Mills, Edward M. Armstrong, and Andrew J. Pershing, *Modeling marine pelagic fish species spatiotemporal distributions utilizing a maximum entropy approach*, *Fisheries Oceanography* **27** (2018), no. 6, 571–586.
- [30] Joseph Rodriguez, Gang Ren, Christopher R. Day, Keji Zhao, Carson C. Chow, and Daniel R. Larson, *Intrinsic dynamics of a human gene reveal the basis of expression heterogeneity*, *Cell* **176** (2019), no. 1, 213 – 226.e18.
- [31] S. Zhu, D. Wang, K. Yu, T. Li, and Y. Gong, *Feature selection for gene expression using model-based entropy*, *IEEE/ACM Transactions on Computational Biology and Bioinformatics* **7** (2010), no. 1, 25–36.
- [32] Noppasit Chakpitak, Paravee Maneejuk, Somsak Chanaim, and Songsak Sriboonchitta, *Thailand in the era of digital economy: How does digital technology promote economic growth?*, *Predictive Econometrics and Big Data (Cham)* (Vladik Kreinovich, Songsak Sriboonchitta, and Nopasit Chakpitak, eds.), Springer International Publishing, 2018, pp. 350–362.
- [33] Mohammad Jahangir, Alam Mumtaz, and Ahmed Ismat Ara Begum, *Nexus between non-renewable energy demand and economic growth in bangladesh: Application of maximum entropy bootstrap approach*, *Renewable and Sustainable Energy Reviews* **72** (2017), 399 – 406.
- [34] A. Talha Yalta, *Analyzing energy consumption and gdp nexus using maximum entropy bootstrap: The case of turkey*, *Energy Economics* **33** (2011), no. 3, 453 – 460.
- [35] J.A. Secrest, J.M. Conroy, and H.G. Miller, *A unified view of transport equations*, *Physica A: Statistical Mechanics and its Applications* **547** (2020), 124403.
- [36] C. E. Shannon, *A mathematical theory of communication*, *The Bell System Technical Journal* **27** (1948), no. 3, 379–423.
- [37] A. R. Plastino, *Tsallis theory, the maximum entropy principle, and evolution equations*, *Nonextensive Statistical Mechanics and Its Applications* (O. Abe and Y. Okamoto, eds.), Springer, Berlin, 2001, pp. 163–191.
- [38] T. Bennett, *Transport by advection and diffusion*, Wiley Global Education, 2012.

- [39] Mahtab Joueiai, J.W.C. Lint, and Serge Hoogendoorn, *Multi-scale traffic flow modeling in mixed networks*, Transportation Research Record Journal of the Transportation Research Board **2421** (2014).
- [40] Champagne, N., Vasseur, R., Montourcy, A., Bartolo, D., 2010. *Traffic jams and intermittent flows in microfluidic networks*, Phys. Rev. Lett. **105**,044502
- [41] Prosenjit Bagchi, *Mesoscale simulation of blood flow in small vessels*, Biophysical Journal **92** (2007), no. 6, 1858 – 1877.
- [42] A. B. Schelin, Gy. Károlyi, A. P. S. de Moura, N. A. Booth, and C. Grebogi, *Chaotic advection in blood flow*, Phys. Rev. E **80** (2009), 016213.
- [43] John David Jackson, *Classical electrodynamics*, 3rd ed. ed., Wiley, New York, NY, 1999.
- [44] Sydney Levitus, *Annual cycle of salinity and salt storage in the world ocean*, Journal of Physical Oceanography **16** (1986), no. 2, 322–343.
- [45] Martin R. Wadley and Grant R. Bigg, *Are “great salinity anomalies” advective?*, Journal of Climate **19** (2006), no. 7, 1080–1088.
- [46] F. A. J. Gifford, *Use of routine meteorological observations for estimating atmospheric dispersion*, vol. 2, 1961, pp. 47–51.
- [47] P Meade and F Pasquill, *A study of the average distribution of pollution around staythorpe*, International journal of air pollution **1** (1958), 60–70.
- [48] F. Pasquill, *The estimation of the dispersion of windborne material*, Meteorology Magazine **90** (1961), 33–40.
- [49] D.B. Turner, *Atmospheric dispersion modeling. a critical review*, J. Air Pollut. Control Assoc.; (United States) **29** (1979), no. 5.
- [50] Kenneth W. Ragland, *Multiple box model for dispersion of air pollutants from area sources*, Atmospheric Environment (1967) **7** (1973), no. 11, 1017 – 1032.
- [51] Kim Seogcheol and Joh Seunghun, *Derivation of new box model to analyze the air pollution trends in a metropolitan area*, Journal of Korean Society for Atmospheric Environment **21** (2005).
- [52] Young-Rae Jung, Warn-Gyu Park, and Ok-Hyun Park, *Pollution dispersion analysis using the puff model with numerical flow field data*, Mechanics Research Communications **30** (2003), no. 4, 277 – 286.
- [53] C. Tsallis, *Possible generalization of boltzmann-gibbs statistics*, Journal of Statistical Physics

- 52** (1988), 479–487.
- [54] G. Kaniadakis, A. M. Scarfone, A. Sparavigna, and T. Wada, *Composition law of κ -entropy for statistically independent systems*, Phys. Rev. E **95** (2017), 052112.
- [55] T Wei, X L Li, and Y S Li, *An inverse time-dependent source problem for a time-fractional diffusion equation*, Inverse Problems **32** (2016), no. 8, 085003.
- [56] J.F. Gómez-Aguilar, M. Miranda-Hernández, M.G. López-López, V.M. Alvarado-Martínez, and D. Baleanu, *Modeling and simulation of the fractional space-time diffusion equation*, Communications in Nonlinear Science and Numerical Simulation **30** (2016), no. 1, 115 – 127.
- [57] Walter Wyss, *The fractional diffusion equation*, Journal of Mathematical Physics **27** (1986), no. 11, 2782–2785.